



Published in final edited form as:

Gastroenterology. 2018 October ; 155(4): 1250–1263.e5. doi:10.1053/j.gastro.2018.06.036.

Transient High Pressure in Pancreatic Ducts Promotes Inflammation and Alters Tight Junctions via Calcineurin Signaling in Mice

Li Wen^{1,*}, Tanveer A. Javed^{1,*}, Dean Yimlamai¹, Amitava Mukherjee¹, Xiangwei Xiao², and Sohail Z. Husain¹

¹Department of Pediatric Gastroenterology, University of Pittsburgh and the Children's Hospital of Pittsburgh of UPMC, Pittsburgh, Pennsylvania, United States

²Department of Surgery, University of Pittsburgh and the Children's Hospital of Pittsburgh of UPMC, Pittsburgh, Pennsylvania, United States

Abstract

Background and aims—Pancreatitis following endoscopic retrograde cholangiopancreatography (PEP) is thought to be provoked by pancreatic ductal hypertension, via unknown mechanisms. We investigated the effects of hydrostatic pressures on the development of pancreatitis in mice.

Methods—We performed studies with Swiss Webster mice, B6129 mice (controls), and B6129 mice with disruption of the protein phosphatase 3, catalytic subunit, beta isoform gene (*Cnab*^{-/-} mice). Acute pancreatitis was induced in mice by retrograde biliopancreatic ductal or intraductal infusion of saline with a constant hydrostatic pressure while the proximal common bile duct was clamped—these mice were used as a model of PEP. Some mice were given pancreatic infusions of AAV6-NFAT-luciferase, to monitor calcineurin activity or the calcineurin inhibitor FK506. Blood samples and pancreas were collected at 6 and 24 hrs and analyzed by ELISA, histology, immunohistochemistry, or fluorescence microscopy. Ca²⁺ signaling and mitochondrial permeability were measured in pancreatic acinar cells isolated 15 min after PEP induction. Ca²⁺-activated phosphatase calcineurin within the pancreas was tracked *in vivo* over 24 hrs.

Results—Intraductal pressures of up to 130 mmHg were observed in the previously reported model of PEP; we found application of hydrostatic pressures of 100 and 150 mmHg for 10 min consistently induced pancreatitis. Pancreatic tissues had markers of inflammation (increased levels

Correspondence: Sohail Z. Husain, MD. Children's Hospital of Pittsburgh, Rangos Research Center, Suite 7123. 4401 Penn Ave, Pittsburgh PA 15224. Phone: 412-692-5412. Fax: 412-692-8907. sohail.husain@chp.edu.

*L.W. and T.A.J. are co-first authors.

Disclosures: The authors declare no conflicts of interest.

Author's contribution: L.W. and S.Z.H. designed the study and obtained funding. L.W. and T.A.J. acquired and analyzed the data. L.W., T.A.J., and S.Z.H. interpreted the data. D.Y., A.M., and X.X. participated in the intellectual discussions. L.W. and S.Z.H. wrote the paper. All authors approved the final edited version.

Publisher's Disclaimer: This is a PDF file of an unedited manuscript that has been accepted for publication. As a service to our customers we are providing this early version of the manuscript. The manuscript will undergo copyediting, typesetting, and review of the resulting proof before it is published in its final citable form. Please note that during the production process errors may be discovered which could affect the content, and all legal disclaimers that apply to the journal pertain.

of interleukin 6 [IL6], IL1B, and tumor necrosis factor [TNF]), activation of STAT3, increased serum amylase and IL6, and loss of tight junction integrity. Transiently high pressures dysregulated Ca²⁺ processing (reduced Ca²⁺ oscillations and an increased peak plateau Ca²⁺ signal) and reduced the mitochondrial membrane potential. We observed activation of pancreatic calcineurin in the pancreas in mice. *Cnab*^{-/-} mice, which lack the catalytic subunit of calcineurin, and mice given FK506 did not develop pressure-induced pancreatic inflammation, edema, or loss of tight junction integrity.

Conclusions—Transient high ductal pressure produces pancreatic inflammation and loss of tight junction integrity in a mouse model of PEP. These processes require calcineurin signaling. Calcineurin inhibitors might be used to prevent acute pancreatitis that results from obstruction.

Keywords

ERCP; signal transduction; calcium; occludin

INTRODUCTION

Post-ERCP (endoscopic retrograde cholangiopancreatography) pancreatitis, or PEP, is a major iatrogenic form of pancreatitis that carries an overall incidence of 10% and a mortality rate of 0.7%¹. Despite some inroads over the last decade in reducing its incidence, the pathogenesis of PEP has remained elusive. We had previously constructed an *in vivo* mouse model of PEP that exploited a combination of chemical injury (with radiocontrast exposure) and ductal hypertension by infusing a large volume of radiocontrast into the pancreatic duct at a high rate². The main issue of the previous work was that radiocontrast exposure was considered by endoscopists as less of a pathogenic factor for PEP compared with pancreatic ductal hypertension. In the current study, we have now focused on pancreatic ductal hypertension in PEP. Although the act of injecting radiocontrast into the pancreatic duct induces an acute rise in pancreatic ductal pressures³ and can be manifested radiographically by the presence of acinarization, most cases of PEP are thought to be caused by a buildup of pancreatic ductal pressures due to pancreatic outflow obstruction from manipulation and subsequent edema of the ampulla of Vater⁴. The evidence for this notion is that, while there are several patient-related risk factors for PEP, most of the risk factors are attributed to procedure-related issues. Some of these procedure-related factors could provoke or worsen the extent of pancreatic outflow obstruction. They include a difficult cannulation, number of cannulation events, cannulation of the pancreatic duct itself, pre-cut sphincterotomy, and ampullectomy⁵.

On a broader level, pancreatic ductal hypertension due to obstruction of the pancreatic duct is likely a shared mechanism for several other etiologies of acute pancreatitis⁶⁻⁹, including the most common etiology, biliary pancreatitis, as well as some of the less frequent causes of pancreatitis, such as from tumors that obstruct the pancreatic duct, from intestinal inflammatory disorders that narrow the ampullary opening, or from double-balloon enteroscopy causing duodenal obstruction^{6, 10}.

In limited experimental animal models, applying hydrostatic pressure caused pancreatitis¹¹⁻¹⁶. However, the signaling events in the pancreas during pancreatic ductal

hypertension are unclear. In the current study we sought to examine the effects of hydrostatic pressures on the development of pancreatitis and the mechanisms through which they mediate pancreatic injury, using a novel *in vivo* mouse model.

We firstly observed a transient elevation of biliopancreatic ductal pressures in a previously reported mouse model of PEP. Based on this information, we generated a pressure-induced pancreatitis model in mice by intraductally delivering constant hydrostatic pressures. We found that applying fixed pressures of 100 mmHg and 150 mmHg for only 10 min induces pancreatitis that is consistently manifested by pancreatic inflammation and the loss of tight junction integrity. Further, we found that transiently high pancreatic ductal pressures caused dysregulation of Ca^{2+} processing and a decrease in mitochondrial membrane potential in isolated pancreatic acinar cells. There was also activation of calcineurin *in vivo*. Genetic or pharmacological inhibition of calcineurin protected against pressure-induced pancreatitis and the loss of tight junction expression, suggesting that calcineurin inhibitors could serve as an effective preventative for the leading obstructive etiologies of acute pancreatitis.

MATERIALS AND METHODS

Reagent and animals

All reagents were purchased from Sigma-Aldrich (St. Louis, MO), unless otherwise specified. Eight to ten-week old mice, weighing 25–30 g and equally divided males and females, were used. The wildtype (WT) mice were of the Swiss Webster strain. The *Cnab* knockout mice were a generous gift of Dr. Jeffery D. Molkentin¹⁷ and were of the B6129 background strain. The controls for the knockout line were sex-, age-, and strain-matched B6129 strain, with similar co-housing conditions. All mice were housed at 22°C with a 12 h light-dark cycle and maintained on standard laboratory chow with free access to food and water. All animal experiments were performed using a protocol approved by the University of Pittsburgh Institutional Animal Care and Use Committee.

Induction of acute pancreatitis

Anesthesia was induced and maintained with 2–4% isoflurane using a vaporizer and gas scavenger system. Using sterile technique, a small midline laparotomy window was created. The distal common bile duct was accessed via a transduodenal puncture and gentle intraluminal cannulation of the ampulla of Vater with a blunt-ended catheter, as previously described^{2, 18–20}. Specifically, the rate-regulated model of PEP was induced by performing retrograde biliopancreatic ductal, or intraductal, infusion of normal saline using a peristaltic rate-regulated pump (Harvard Apparatus, Holliston, MA). While the proximal common bile duct was clamped so that the infusate flowed only into the pancreas. The pressure-regulated mode of PEP was similarly induced by infusing normal saline into the biliopancreatic duct, but infusion was achieved using a hydrostatic pressure-regulated pump (PHD ULTRA™ constant pressure syringe pump, Harvard Apparatus, Holliston, MA). Intraductal pressures were monitored using an APT300 pressure transducer (Harvard Apparatus, Holliston, MA). Buprenorphine analgesia (0.05 mg/kg, ip) was given immediately after surgery, and the mice

were subsequently monitored for physical activity, grooming routines, level of alertness, response to stimulation, and other signs of distress.

Serum amylase and interleukin 6 measurements

Early blood collections (6 h post-pancreatitis induction) were obtained by submandibular bleeding. Serum was obtained by centrifuging the blood at $1,500 \times g$ for 10 min at 4°C . Serum amylase was measured using a Phadebas Kit (Amersham Pharmacia, Rochester, NY). Later blood collections (24 h post-induction) were obtained during a terminal bleeding. At this time point, interleukin 6 (IL6) was measured using a standard enzyme-linked immunosorbent assay (Biolegend, San Diego, CA).

Histology, edema analysis, and immunohistochemistry

The pancreas, duodenum, and spleen were placed en bloc in a cassette in order to maintain its anatomical orientation. The tissues were fixed in 10% formalin at room temperature for 24 h. Paraffin-embedded sections were stained with hematoxylin and eosin (H&E). Ten systematically selected fields at 200X magnification were graded in a blinded fashion from the head of the pancreas, which was identified by its juxtaposition to the duodenum. The subjective grading score gave equal weight (from 0 to 3) for edema, inflammatory infiltration, and necrosis, as previously described²¹. Edema indices were further delineated objectively by performing objective intensity thresholding using ImageJ software (NIH, Bethesda, MD), as previously described^{20, 22}. Briefly, at least 5 images from each slide were selected for the analysis. Areas within the parenchyma were demarcated through low pixel intensity thresholding as edema, and their surface area was calculated as a percentage of the total parenchymal area. Immunohistochemistry for the pan-leukocyte marker CD45 was performed on paraffin-embedded pancreatic tissue sections after xylene deparaffinization, graded ethanol re-hydration, and antigen retrieval. Endogenous peroxidase was blocked with 3% hydrogen peroxide. Primary antibody of rat anti-mouse CD45 (1:100, Becton-Dickinson Biosciences, Franklin Lakes, NJ) was incubated overnight and visualized using a biotin immunoenzymatic antigen detection system (Vector Laboratories, Burlingame, CA).

Isolation of pancreatic acinar cells and confocal imaging

Mouse pancreatic acinar cells were isolated as previously described^{2, 23}, with minor modifications. Briefly, the pancreas was removed and washed with PBS. The head of the pancreas was first identified based on its proximity to the duodenum (Figure 4A). It was then carefully resected and incubated with 2 mg/mL type-4 collagenase (Worthington, Freehold, NJ) for 20 min at 37°C . The pancreatic acinar cells were subsequently isolated by mechanical disruption of the tissue, then filtered through a $70 \mu\text{m}$ cell strainer (Corning, Corning, NY), and centrifuged at 1,000 rpm for 1 min. The pellet was resuspended in extracellular buffer containing 10 mmol/L HEPES (pH 7.3), 10 mmol/L D-glucose, 140 mmol/L NaCl, 4.7 mmol/L KCl, 1.13 mmol/L MgCl_2 , and 1.2 mmol/L CaCl_2 . To assess cytosolic Ca^{2+} signals, the cells were loaded with the high-affinity Ca^{2+} dye Fluo-4AM (4 $\mu\text{mol/L}$) at room temperature for 30 min. They were placed on a perfusion chamber and imaged using an LSM710 laser scanning confocal microscope (Carl Zeiss, Jena, Germany). The Fluo-4AM dye was excited at a wavelength of 488 nm, and emission signals greater than 515 nm were collected every 2 s. Ca^{2+} signals were monitored firstly at baseline for 60

s and then stimulated with a submaximal concentration of the muscarinic agonist carbachol (CCh, 100 nM). To assess mitochondrial membrane potential, the cells were loaded with tetramethylrhodamine methyl ester (TMRM, 50 nmol/L) at room temperature for 30–45 min. The TMRM dye was excited at a wavelength of 543 nm, and emission signals greater than 550 nm were collected every 5 s. The mitochondrial membrane potential was monitored firstly for 450 s and then the protonophore carbonyl cyanide m-chlorophenyl hydrazone (CCCP) was applied to dissipate mitochondrial membrane potential as a positive control. Analysis of the recordings was performed using ImageJ software (National Institute of Health, Bethesda, MD), and fluorescence intensity (F) for each cell was normalized to the baseline fluorescence (F_0) and represented as F/F_0 .

Statistical analysis

Data were expressed as mean \pm SEM, unless otherwise specified. Statistical analysis was performed using GraphPad Prism 6 (GraphPad, La Jolla, CA). Comparisons between groups were performed using ANOVA. A p value of less than 0.05 was considered statistically significant.

RESULTS

High intraductal pressures are observed in a model of obstructive acute pancreatitis

To assess the magnitude of the intraductal pressures in a mouse model of obstructive pancreatitis, we performed a transduodenal cannulation of the distal biliopancreatic duct (Figure 1A). The cannula was attached to a rate-regulated infusion pump, along with a pressure transducer. The obstructive model for PEP was induced by infusing normal saline at a high rate of 20 $\mu\text{L}/\text{min}^2$.²⁰ This model mimics the back flow of pancreatic juice due to edema at the ampulla of Vater during the ERCP, and it induces pancreatitis that is restricted to the head of the pancreas. A low infusion rate of 2–5 $\mu\text{L}/\text{min}$ was infused in a comparator arm, and these control mice failed to develop pancreatitis^{2, 20}. The peak intraductal pressure achieved during the high infusion rate was 130 mmHg, compared with 20–40 mmHg in the negative control (Figure 1B). Upon stopping the infusion, the pressures dropped within 3 min to 40 mmHg for the high infusion rate model and within 1 min to 20 mmHg for the low infusion rate. These data suggest that transiently high intraductal pressures are observed in a rate-infusion model of PEP.

Transiently intraductal application of constant hydrostatic pressures induces pancreatitis

Since we observed transient, high intraductal pressures in the above model of obstructive acute pancreatitis, we next examined whether applying constant hydrostatic pressures influenced the development or severity of acute pancreatitis. Using a pressure-regulated pump, along with the pressure transducer (Figure 2A), we found that 50 mmHg hydrostatic pressure for 10 min caused minimal pancreatic histological damage 24 h after induction. However, raising the hydrostatic pressure to 100 mmHg or 150 mmHg resulted in substantially greater histological damage ($p < 0.05$, Figure 2B). We consistently observed similar pressure-dependent changes in edema thresholding (Figure 2C), subscore for inflammatory infiltrate (additionally assessed by CD45 immunostaining; Figure 2D), and necrosis (Figure 2E). Further, serum amylase at 6 h and IL6 at 24 h after pancreatitis

induction were markedly elevated (Figure 2F, G). These data demonstrate that transiently high, constant hydrostatic pressures induce pancreatitis, suggesting that increased intraductal pressure is an important initiator of PEP.

Pressure-induced pancreatitis leads to elevated proinflammatory signals and altered tight junction integrity

Since the inflammatory response is a critical determinant of pancreatitis severity after pancreatitis initiation^{24, 25}, we characterized pancreatic proinflammatory signals in PIP 24 h after pressure induction. With increasing intraductal pressures, expression of the proinflammatory cytokines IL6, IL1B, and TNF from the pancreatic head was upregulated (Figure 3A). On IL6 target cells, IL6 is known to transmit signals through Janus kinase 2-mediated phosphorylation of the signal transducer and activator transcription 3 (STAT3) at Y705²⁶. IL-6 trans-signaling via STAT3 has also been shown to mediate severe acute pancreatitis and pancreatitis-associated lung injury²⁷. We found that expression of p-STAT3 at Y705 was significantly increased with high pressures (Figure 3B), suggesting that IL-6 trans-signaling within the pancreas is activated during pressure-induced pancreatitis.

We next examined whether increased pancreatic ductal pressure causes transgression of the epithelial barrier and increased ductal permeability. An important determinant of epithelial barrier function and paracellular permeability is the maintenance of intercellular tight junction expression^{28, 29}. Tight junctions are comprised of a complex of proteins, including occludin and zonula occludens (ZO). We found that with high intraductal pressures, the expression of the tight junction genes occludin, ZO1, and ZO2, from the pancreatic head at 24 h, was downregulated (Figure 3C), suggesting that altered tight junction integrity is associated with pressure-induced pancreatitis.

Pressure-induced pancreatitis leads to dysregulation of pancreatic acinar Ca²⁺ processing and a decrease in mitochondrial membrane potential

Aberrant pancreatic acinar Ca²⁺ signals are an early and critical feature of virtually every form of pancreatitis, including post-ERCP pancreatitis and biliary acute pancreatitis^{2, 23, 30–33}. Also, early changes in pancreatic acinar Ca²⁺ signals have been reported in a rodent model of pancreatic duct obstruction³⁴. The resulting ductal hypertension was inferred to have occurred, as a result of complete pancreatic duct obstruction in this ligation models, but due to technical issues with pressure monitoring, direct measurements of ductal pressure could not be performed. Hence, in the current study, we examined whether hydrostatic pressures affect pancreatic acinar Ca²⁺ processing. We isolated pancreatic acinar cells from the head of the pancreas 15 min after applying a hydrostatic pressure of 150 mmHg (Figure 4A). The cells were then stimulated with the muscarinic agonist carbachol (CCh) at a concentration (100 nM) that is known to cause Ca²⁺ oscillations in most of the healthy control acinar cells³⁵. In acinar cells from sham-operated mice, we observed the following five patterns of Ca²⁺ responses: (1) As expected, most cells had oscillations, which were manifested as two or more Ca²⁺ spikes that returned to the baseline and in which the amplitude was at least two times higher than the baseline; (2) A few cells had non-oscillations, which were defined as a single Ca²⁺ spike that returned to the baseline and in which the amplitude was two times higher than the baseline; (3) A peak-

plateau, which were Ca^{2+} signals in which the amplitude of the peak was two times greater than the baseline, but the tracing did not return to baseline within 60 s from the time of the peak signal; (4) A minimal response, which were Ca^{2+} spikes, however, with an amplitude that failed to rise two times above the baseline; (5) No response, which were no appreciable Ca^{2+} spikes throughout the recording (Supplementary Figure 1A). In contrast to the Ca^{2+} signals from the sham group, the acinar cells from mice that received high ductal pressures had a marked reduction in Ca^{2+} oscillations, down from 62.1% to 26%, and an increase in the pathological peak-plateau Ca^{2+} signal, up from 4.7% to 22.7% (Figure 4B), suggesting that hydrostatic pressures predispose pancreatic acinar cells to a sustained, pathological Ca^{2+} signal. Upon further comparing the shape of the peak-plateau Ca^{2+} signals between the sham and pressure induction, there was a slower decay in cytosolic Ca^{2+} (at 150 s from the start of the recording) in the cells from the pressure-induced mice (Supplementary Figure 1A, B). However, the overall intracellular Ca^{2+} load, assessed by the area under the curve in the composite tracings, remained unchanged (Supplementary Figure 1C). The findings suggest that intraductal pressure causes delayed acinar cell Ca^{2+} extrusion, likely due to an impairment of the plasma membrane Ca^{2+} ATPase (PMCA). Since acute mitochondrial dysfunction has been implicated in numerous experimental models of acute pancreatitis^{36–38}, we next assessed the impact of intraductal pressure on mitochondrial permeability. We found that transiently high intraductal pressure induces a significant decrease in mitochondrial membrane potential, which likely results in blunting ATP production (Figure 4C). These data suggest that early dysregulation of pancreatic acinar Ca^{2+} processing and a decrease of mitochondrial permeability occurs early during pressure-induced pancreatitis.

Pressure-induced pancreatitis causes pancreatic calcineurin activation

A potent target of the aberrant acinar Ca^{2+} signals during pancreatitis is the Ca^{2+} -activated phosphatase calcineurin^{2, 39, 40}. Since we observed early changes of pancreatic Ca^{2+} processing during pressure induction, we examined whether hydrostatic pressures cause the activation of pancreatic calcineurin. NFAT (nuclear factor of activated T-cells), which translocates into the nucleus upon dephosphorylation by calcineurin in the cytosol, is a surrogate marker for assessing calcineurin activation^{2, 40–42}. Thus, we generated an AAV6-NFAT-luciferase to dynamically monitor *in vivo* activation of calcineurin (Figure 5A). We monitored pancreas-specific calcineurin activation by intraductally infusing the AAV6-NFAT-luciferase into the pancreas (Figure 5B). During pressure induction with 150 mmHg, we observed that the NFAT bioluminescence signals increased 10-fold above baseline 4 h after induction, peaked at 23-fold above baseline at 8 h, and returned to baseline 24 h later (Figure 5C). By contrast, there was no elevation of pancreatic NFAT signals throughout this time frame in the sham or the lower pressure condition. The findings suggest that high pancreatic ductal pressures cause abnormal acinar Ca^{2+} processing and calcineurin activation in the pancreas. We next evaluated the effects of ductal pressure on mitochondrial permeability in acinar cells from pressure-induced *Cnab* knockout mice, which lack the predominant catalytic subunit of calcineurin¹⁷. We found that, compared to the WT, *Cnab* knockouts had a similar decrease in mitochondrial permeability (Supplementary Figure 2).

Genetic and pharmacological inhibition of calcineurin protects against pressure-induced pancreatitis

To determine whether the increase in calcineurin activation mediates pressure-induced pancreatitis, we tested (1) mice with a genetic deletion of *Cnab*, a predominant catalytic subunit of calcineurin in acinar cells, and (2) WT mice that were treated with the highly specific calcineurin inhibitor, FK506. Compared to age- and sex-matched WT controls, we found that *Cnab* knockout mice had a near-complete reduction in histological damage, including each of the subscores for edema assessed by image thresholding, inflammatory infiltrate (additionally examined by CD45 immunostaining), necrosis, and serum IL6. Serum amylase was, however, not reduced with this genetic strain (Figure 6A, B and Supplementary Figure 3). Systemic administration of FK506 (1 mg/kg) to WT mice reduced histological severity by 50% down to the sham condition. Serum amylase at 6 h and IL6 at 24 h were similarly reduced (Figure 6C–E and Supplementary Figure 4).

Since we observed that high intraductal pressures cause upregulation of pancreatic inflammatory genes and the loss of tight junction integrity in the pancreas, we assessed whether one or both parameters are mediated through calcineurin. We found that either genetic deletion of calcineurin or application of FK506 abrogated the upregulation of pancreatic proinflammatory cytokine expression and also prevented phosphorylation of STAT3 at Y705 (Figure 7A–D). The expression of the tight junction genes occludin, ZO1, and ZO2, was largely preserved in the *Cnab* knockouts that underwent pressure induction, and there was a partial, albeit significant, trend towards preventing the reduction with FK506 (Figure 7E, F). These data suggest that calcineurin signaling is a critical downstream mediator of both pancreatic inflammation and loss of tight junction integrity during pressure-induced pancreatitis.

DISCUSSION

Our previously constructed *in vivo* mouse model of PEP exploited both chemical injury and pancreatic ductal hypertension by infusing a large volume of radiocontrast into the pancreatic duct at a high rate. Although not quantified at the time of the report², the pancreatic ductal pressures were estimated to be transiently elevated in this model. We found that mice with a genetic deletion of calcineurin (either globally² or selectively within the acinar cells²⁰) or wildtype mice receiving calcineurin inhibitors protected against this form of PEP. In isolated acinar cells, we found that radiocontrast had induced cell injury through calcium and calcineurin signaling².

In this study, we focused on the role of pancreatic ductal hypertension on the development of PEP. We began by evaluating the intraductal pressures that were induced in the previously reported mild model of PEP², in which, rather than radiocontrast, an intraductal bolus of normal saline was infused via a rate-regulated pump over a period of 5–10 minutes. In this setting, we observed transiently increased pressures of up to 130 mmHg, compared with an intraductal pressure of 20–40 mmHg in the control animals. Given the small biliopancreatic duct diameter of the mouse in relation to that of the catheter and the need to infuse at least 1–5 μ L per minute of fluid to reliably detect intraductal pressures, the basal pressures we recorded likely overestimate native ductal pressures. Nonetheless, the basal pressures we

observed in the mouse were still in the same range seen in healthy people during ERCP³. We have also presumed that the pressures in the distal common bile duct, where the pressure transducer was placed, were equilibrated with the pressures in the main pancreatic duct of the mouse, since there was visibly a free flow of fluid between the ducts and, unlike in humans³, in mice there are by histology no smooth muscle sphincters at the junction of the common bile duct and pancreatic duct⁴³.

The high intraductal pressures we have induced in this model of PEP meant to mimic the pressures that develop after an ERCP, due to transient edema at the ampulla of Vater and consequent backup of pancreatic juice. While there are multiple reports of monitoring ductal pressures during ERCP in patients, no one has yet been able to measure pancreatic ductal pressures after ERCP. For this reason, there is currently no way of knowing how the ductal pressures we induced in mice compared to the ductal pressures achieved after ERCP in humans. In the future, there may be non-invasive imaging methods of tracking these ductal pressure changes in the clinical setting over time after the ERCP.

Based on the pressures we recorded using the rate-regulated normal saline infusion model, we subsequently generated a model of pressure-induced pancreatitis by delivering normal saline via a pressure-regulated pump for a brief period of 10 min at pressures at or above 100 mmHg. Although infusing at a hydrostatic pressure of 50 mmHg caused some degree of pancreatic inflammatory gene upregulation, the higher pressures induced a much greater degree of pancreatic edema, inflammatory infiltrate, and necrosis. The pancreatic damage was also associated with a drop in tight junction expression. This is consistent with studies in rats¹¹ and cats¹², in which applying hydrostatic pressure led to increased permeability and leakage of the infusion fluid into the interstitium. The current study did not examine the impact of intraductal pressure on pancreatic ductal function, a primary feature of which is to alkalize pancreatic juice. However, the pancreatic ductal cells exert a role in pancreatitis^{44, 45}. Takacs et al. showed that elevated intraductal pressure in the setting of pancreatitis was associated with intraductal acidosis⁴⁶. Intraductal pH was shown in some studies to affect pancreatitis severity. Noble et al. described a pH-sensitive neurogenic pathway that can mediate pancreatic inflammation in a PEP model in rats¹⁶. In our previous study of PEP in mice², we did not observe differences in PEP outcome using a buffered infusate of pH 6.0, compared to a control of pH 7.3. Further studies are required to probe the direct effects of ductal hypertension on pancreatic ductal function and intraductal acidosis during PEP.

Aberrant Ca²⁺ signals, defined as high amplitude, non-oscillatory, sustained peak-plateau Ca²⁺ signals are an early and critical mediator of acute pancreatitis. Early changes in Ca²⁺ signaling in response to submaximal secretagogue stimulation were observed after pancreatic duct ligation in rodents³⁴. In this ligation model, there was a rise, within 4 h, of trypsinogen activation peptide, a marker of trypsin activation. The elevation was largely prevented by *in vivo* calcium chelation, suggesting that ductal pressure-induced trypsin activation is calcium-dependent. We also observed an increase in the proportion of peak-plateau Ca²⁺ signals from pancreatic acinar cells isolated within 15 min of pressure induction. Moreover, we observed that the shape of the peak-plateau Ca²⁺ signals in the cells from the pressure-induced mice manifested a slow return from their peak levels, implying an

impairment of Ca^{2+} extrusion. In pancreatic acinar cells, Ca^{2+} extrusion is primarily conducted by the PMCA⁴⁷⁻⁵⁰. Impaired PMCA function could indirectly result from acute mitochondrial depolarization and ATP depletion, since PMCA is ATP-dependent. There is evidence for acute mitochondrial dysfunction in numerous experimental models of acute pancreatitis³⁶⁻³⁸, and we also found intraductal pressure induces a decrease in mitochondrial membrane potential, which is likely responsible for blunting ATP production. Or there could be a more direct impact of hydrostatic pressure on PMCA activity, as demonstrated with PMCA purified from erythrocytes⁵¹. The mechanism by which intraductal pressure induces pancreatic Ca^{2+} toxicity is unclear and will require further studies that probe the contribution of an array of recently characterized plasma membrane-bound mechanotransducer channels, which are capable of conducting ion flux in response to mechanical stimuli^{52, 53}. A recent study by Romac and colleagues suggests a role of the mechanically activated Piezo1 channel in pressure-induced pancreatitis⁵⁴.

Calcineurin is a potent downstream target of Ca^{2+} and has been implicated as a critical mediator of acinar injury and pancreatitis *in vivo*^{20, 40, 55}. The pancreatic acinar cell primarily expresses the *Cnab* and CnB1 isoforms of calcineurin⁵⁶. We found that high pancreatic ductal pressures mediate pressure-induced pancreatitis through calcineurin activation and that calcineurin deletion (using *Cnab* knockouts) or calcineurin inhibition (with FK506) largely prevents pancreatic inflammation and the loss of tight junction expression. We observed a similar decrease in mitochondrial membrane potential in *Cnab* knockouts early after pressure induction, indicating that calcineurin activation is either downstream to or independent of pressure-induced mitochondrial depolarization.

In summary, we observed high intraductal pressures in a previously reported rate-regulated intraductal infusion model of PEP. We found that transiently inducing high hydrostatic pressures using a pressure-regulated pump results in consistent and graded pancreatitis. Pressure-induced pancreatitis was associated with substantial pancreatic inflammation and the loss of tight junction integrity. Both of the pathological aspects induced by pancreatic ductal hypertension were mediated through calcineurin signaling.

The findings suggest that calcineurin inhibitors could serve as an effective preventative for the common scenario of PEP which results from increased pancreatic ductal pressures, even in the absence of radiocontrast exposure. More broadly, studying the role of the Ca^{2+} /calcineurin signaling pathway in the pressure-induced form of PEP could provide insight into potential therapies for other obstructive etiologies of pancreatitis and pressure-associated injury.

Supplementary Material

Refer to Web version on PubMed Central for supplementary material.

Acknowledgments

Grant support: This work was supported by National Institutes of Health Grants DK093491 and DK103002 (to S.Z.H.) and a Children's Hospital of Pittsburgh of UPMC Foundation Grant (to L.W.).

Abbreviations

AAV	adeno-associated virus
CCCP	carbonyl cyanide m-chlorophenyl hydrazine
ERCP	endoscopic retrograde cholangiopancreatography
H&E	hematoxylin and eosin
IL	interleukin
ip	intraperitoneal
ITR	inverted terminal repeat
Luc 2P	luciferase 2P
MP	minimal promoter
NFAT	nuclear factor of activated T-cells
pA	poly A
PEG	polyethylene glycol
PEP	post-ERCP pancreatitis
PMCA	plasma membrane Ca ²⁺ ATPase
RE	response element
RT-qPCR	reverse transcription quantitative polymerase chain reaction
SERCA	sarco(endo)plasmic reticulum Ca ²⁺ -activated ATPase
STAT3	signal transducer and activator transcription 3
TMRM	tetramethyl rhodamine methyl ester
TNF	tumor necrosis factor
WT	wildtype
ZO	zonula occludens

References

1. Kochar B, Akshintala VS, Afghani E, et al. Incidence, severity, and mortality of post-ERCP pancreatitis: a systematic review by using randomized, controlled trials. *Gastrointest Endosc.* 2015; 81:143–149. e9. [PubMed: 25088919]
2. Jin S, Orabi AI, Le T, et al. Exposure to Radiocontrast Agents Induces Pancreatic Inflammation by Activation of Nuclear Factor-kappaB, Calcium Signaling, and Calcineurin. *Gastroenterology.* 2015; 149:753–64. e11. [PubMed: 25980752]

3. Csendes A, Kruse A, Funch-Jensen P, et al. Pressure measurements in the biliary and pancreatic duct systems in controls and in patients with gallstones, previous cholecystectomy, or common bile duct stones. *Gastroenterology*. 1979; 77:1203–10. [PubMed: 499707]
4. Thaker AM, Mosko JD, Berzin TM. Post-endoscopic retrograde cholangiopancreatography pancreatitis. *Gastroenterol Rep (Oxf)*. 2015; 3:32–40. [PubMed: 25406464]
5. Chandrasekhara V, Khashab MA, et al. Committee ASoP. Adverse events associated with ERCP. *Gastrointest Endosc*. 2016
6. Forsmark CE, Vege SS, Wilcox CM. Acute Pancreatitis. *N Engl J Med*. 2016; 375:1972–1981. [PubMed: 27959604]
7. Lerch MM, Weidenbach H, Hernandez CA, et al. Pancreatic outflow obstruction as the critical event for human gall stone induced pancreatitis. *Gut*. 1994; 35:1501–3. [PubMed: 7959214]
8. Lerch MM, Saluja AK, Runzi M, et al. Pancreatic duct obstruction triggers acute necrotizing pancreatitis in the opossum. *Gastroenterology*. 1993; 104:853–61. [PubMed: 7680018]
9. Siqin D, Wang C, Zhou Z, et al. The key event of acute pancreatitis: pancreatic duct obstruction and bile reflux, not a single one can be omitted. *Med Hypotheses*. 2009; 72:589–91. [PubMed: 19147295]
10. Chavalitdhamrong D, Adler DG, Draganov PV. Complications of enteroscopy: how to avoid them and manage them when they arise. *Gastrointest Endosc Clin N Am*. 2015; 25:83–95. [PubMed: 25442960]
11. Armstrong CP, Taylor TV, Torrance HB. Pressure, volume and the pancreas. *Gut*. 1985; 26:615–24. [PubMed: 2408971]
12. Harvey MH, Wedgwood KR, Austin JA, et al. Pancreatic duct pressure, duct permeability and acute pancreatitis. *Br J Surg*. 1989; 76:859–62. [PubMed: 2475200]
13. Pirola RC, Davis AE. Effect of pressure on the integrity of the duct-acinar system of the pancreas. *Gut*. 1970; 11:69–73. [PubMed: 5435271]
14. Bozkurt S, Guner A, Kadioglu H, et al. The effects of different mechanisms on the development of post-ERCP pancreatitis in an ERCP model in rats. *Turk J Gastroenterol*. 2013; 24:469–75. [PubMed: 24623284]
15. Haciahmetoglu T, Ertekin C, Dolay K, et al. The effects of contrast agent and intraductal pressure changes on the development of pancreatitis in an ERCP model in rats. *Langenbecks Arch Surg*. 2008; 393:367–72. [PubMed: 17674029]
16. Noble MD, Romac J, Vigna SR, et al. A pH-sensitive, neurogenic pathway mediates disease severity in a model of post-ERCP pancreatitis. *Gut*. 2008; 57:1566–71. [PubMed: 18625695]
17. Bueno OF, Brandt EB, Rothenberg ME, et al. Defective T cell development and function in calcineurin A beta -deficient mice. *Proc Natl Acad Sci U S A*. 2002; 99:9398–403. [PubMed: 12091710]
18. Perides G, van Acker GJ, Laukkarinen JM, et al. Experimental acute biliary pancreatitis induced by retrograde infusion of bile acids into the mouse pancreatic duct. *Nat Protoc*. 2010; 5:335–41. [PubMed: 20134432]
19. Le T, Eisses JF, Lemon KL, et al. Intraductal infusion of taurocholate followed by distal common bile duct ligation leads to a severe necrotic model of pancreatitis in mice. *Pancreas*. 2015; 44:493–9. [PubMed: 25469547]
20. Orabi AI, Wen L, Javed TA, et al. Targeted inhibition of pancreatic acinar cell calcineurin is a novel strategy to prevent post-ERCP pancreatitis. *Cell Mol Gastroenterol Hepatol*. 2017; 3:119–128. [PubMed: 28090570]
21. Wildi S, Kleeff J, Mayerle J, et al. Suppression of transforming growth factor beta signalling aborts caerulein induced pancreatitis and eliminates restricted stimulation at high caerulein concentrations. *Gut*. 2007; 56:685–92. [PubMed: 17135311]
22. Kim MS, Hong JH, Li Q, et al. Deletion of TRPC3 in mice reduces store-operated Ca²⁺ influx and the severity of acute pancreatitis. *Gastroenterology*. 2009; 137:1509–17. [PubMed: 19622358]
23. Wen L, Voronina S, Javed MA, et al. Inhibitors of ORAI1 Prevent Cytosolic Calcium-associated Injury of Human Pancreatic Acinar Cells and Acute Pancreatitis in 3 Mouse Models. *Gastroenterology*. 2015

24. Pandol SJ, Saluja AK, Imrie CW, et al. Acute pancreatitis: bench to the bedside. *Gastroenterology*. 2007; 132:1127–51. [PubMed: 17383433]
25. Petrov MS, Shanbhag S, Chakraborty M, et al. Organ failure and infection of pancreatic necrosis as determinants of mortality in patients with acute pancreatitis. *Gastroenterology*. 2010; 139:813–20. [PubMed: 20540942]
26. Jones SA, Richards PJ, Scheller J, et al. IL-6 transsignaling: the in vivo consequences. *J Interferon Cytokine Res*. 2005; 25:241–53. [PubMed: 15871661]
27. Zhang H, Neuhofer P, Song L, et al. IL-6 trans-signaling promotes pancreatitis-associated lung injury and lethality. *J Clin Invest*. 2013; 123:1019–31. [PubMed: 23426178]
28. Turner JR. Intestinal mucosal barrier function in health and disease. *Nat Rev Immunol*. 2009; 9:799–809. [PubMed: 19855405]
29. Sharma D, Malik A, Guy CS, et al. Pyloric Inflammation Regulates Tight Junction Integrity to Restrict Colitis and Tumorigenesis. *Gastroenterology*. 2017
30. Ward JB, Sutton R, Jenkins SA, et al. Progressive disruption of acinar cell calcium signaling is an early feature of cerulein-induced pancreatitis in mice. *Gastroenterology*. 1996; 111:481–91. [PubMed: 8690215]
31. Criddle DN, Murphy J, Fistetto G, et al. Fatty acid ethyl esters cause pancreatic calcium toxicity via inositol trisphosphate receptors and loss of ATP synthesis. *Gastroenterology*. 2006; 130:781–93. [PubMed: 16530519]
32. Voronina S, Longbottom R, Sutton R, et al. Bile acids induce calcium signals in mouse pancreatic acinar cells: implications for bile-induced pancreatic pathology. *J Physiol*. 2002; 540:49–55. [PubMed: 11927668]
33. Ward JB, Petersen OH, Jenkins SA, et al. Is an elevated concentration of acinar cytosolic free ionized calcium the trigger for acute pancreatitis? *Lancet*. 1995; 346:1016–9. [PubMed: 7475553]
34. Mooren F, Hlouschek V, Finkes T, et al. Early changes in pancreatic acinar cell calcium signaling after pancreatic duct obstruction. *J Biol Chem*. 2003; 278:9361–9. [PubMed: 12522141]
35. Luo X, Shin DM, Wang X, et al. Aberrant localization of intracellular organelles, Ca²⁺ signaling, and exocytosis in Mist1 null mice. *J Biol Chem*. 2005; 280:12668–75. [PubMed: 15665001]
36. Shalbueva N, Mareninova OA, Gerloff A, et al. Effects of oxidative alcohol metabolism on the mitochondrial permeability transition pore and necrosis in a mouse model of alcoholic pancreatitis. *Gastroenterology*. 2013; 144:437–446. e6. [PubMed: 23103769]
37. Mukherjee R, Mareninova OA, Odinkova IV, et al. Mechanism of mitochondrial permeability transition pore induction and damage in the pancreas: inhibition prevents acute pancreatitis by protecting production of ATP. *Gut*. 2015
38. Biczó G, Vegh ET, Shalbueva N, et al. Mitochondrial Dysfunction, Through Impaired Autophagy, Leads to Endoplasmic Reticulum Stress, Deregulated Lipid Metabolism, and Pancreatitis in Animal Models. *Gastroenterology*. 2018; 154:689–703. [PubMed: 29074451]
39. Husain SZ, Grant WM, Gorelick FS, et al. Cerulein-induced intracellular pancreatic zymogen activation is dependent on calcineurin. *Am J Physiol Gastrointest Liver Physiol*. 2007; 292:G1594–9. [PubMed: 17332472]
40. Muili KA, Wang D, Orabi AI, et al. Bile acids induce pancreatic acinar cell injury and pancreatitis by activating calcineurin. *J Biol Chem*. 2013; 288:570–80. [PubMed: 23148215]
41. Wilkins BJ, Dai YS, Bueno OF, et al. Calcineurin/NFAT coupling participates in pathological, but not physiological, cardiac hypertrophy. *Circ Res*. 2004; 94:110–8. [PubMed: 14656927]
42. Peucker K, Muff S, Wang J, et al. Epithelial calcineurin controls microbiota-dependent intestinal tumor development. *Nat Med*. 2016; 22:506–15. [PubMed: 27043494]
43. Higashiyama H, Sumitomo H, Ozawa A, et al. Anatomy of the Murine Hepatobiliary System: A Whole-Organ-Level Analysis Using a Transparency Method. *Anat Rec (Hoboken)*. 2016; 299:161–72. [PubMed: 26559382]
44. Hegyi P, Petersen OH. The exocrine pancreas: the acinar-ductal tango in physiology and pathophysiology. *Rev Physiol Biochem Pharmacol*. 2013; 165:1–30. [PubMed: 23881310]
45. Hegyi P, Rakonczay Z Jr. The role of pancreatic ducts in the pathogenesis of acute pancreatitis. *Pancreatol*. 2015

46. Takacs T, Rosztoczy A, Maleth J, et al. Intraductal acidosis in acute biliary pancreatitis. *Pancreatology*. 2013; 13:333–5. [PubMed: 23890129]
47. Bruce JI, Elliott AC. Oxidant-impaired intracellular Ca²⁺ signaling in pancreatic acinar cells: role of the plasma membrane Ca²⁺-ATPase. *Am J Physiol Cell Physiol*. 2007; 293:C938–50. [PubMed: 17494627]
48. Mankad P, James A, Siriwardena AK, et al. Insulin protects pancreatic acinar cells from cytosolic calcium overload and inhibition of plasma membrane calcium pump. *J Biol Chem*. 2012; 287:1823–36. [PubMed: 22128146]
49. Petersen OH, Sutton R. Ca²⁺ signalling and pancreatitis: effects of alcohol, bile and coffee. *Trends Pharmacol Sci*. 2006; 27:113–20. [PubMed: 16406087]
50. Li J, Zhou R, Zhang J, et al. Calcium signaling of pancreatic acinar cells in the pathogenesis of pancreatitis. *World J Gastroenterol*. 2014; 20:16146–52. [PubMed: 25473167]
51. Coelho-Sampaio T, Ferreira ST, Benaim G, et al. Dissociation of purified erythrocyte Ca(2+)-ATPase by hydrostatic pressure. *J Biol Chem*. 1991; 266:22266–72. [PubMed: 1834668]
52. Delmas P, Hao J, Rodat-Despoix L. Molecular mechanisms of mechanotransduction in mammalian sensory neurons. *Nat Rev Neurosci*. 2011; 12:139–53. [PubMed: 21304548]
53. James SL. Molecules pressured to react. *Nature*. 2018; 554:468–469. [PubMed: 29469128]
54. Romac JM, Shahid RA, Swain SM, et al. Piezo1 is a mechanically activated ion channel and mediates pressure induced pancreatitis. *Nat Commun*. 2018; 9:1715. [PubMed: 29712913]
55. Shah AU, Sarwar A, Orabi AI, et al. Protease activation during in vivo pancreatitis is dependent on calcineurin activation. *Am J Physiol Gastrointest Liver Physiol*. 2009; 297:G967–73. [PubMed: 20501444]
56. Orabi AI, Luo Y, Ahmad MU, et al. IP3 receptor type 2 deficiency is associated with a secretory defect in the pancreatic acinar cell and an accumulation of zymogen granules. *PLoS One*. 2012; 7:e48465. [PubMed: 23185258]

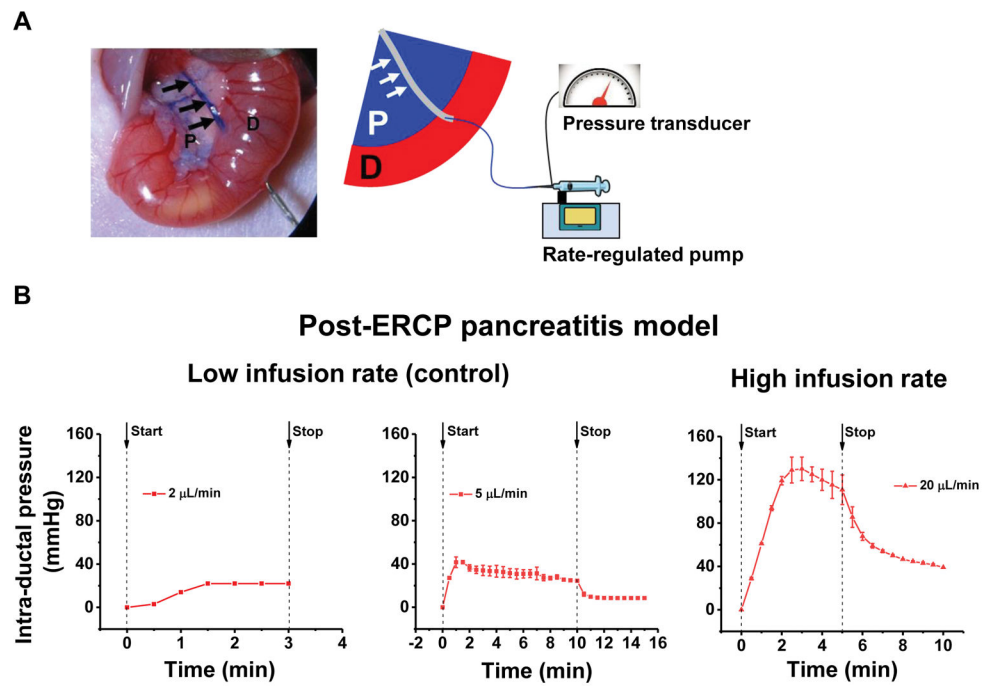


Figure 1. High intraductal pressures are observed in an experimental mouse model of post-ERCP pancreatitis (PEP)

(A) A schematic of the rate-regulated pump with pressure monitoring. P, pancreas; D, duodenum. (B) Pressures observed with low (negative control) or high intraductal infusion of normal saline. The arrows point to the time of the start or stop of the infusion.

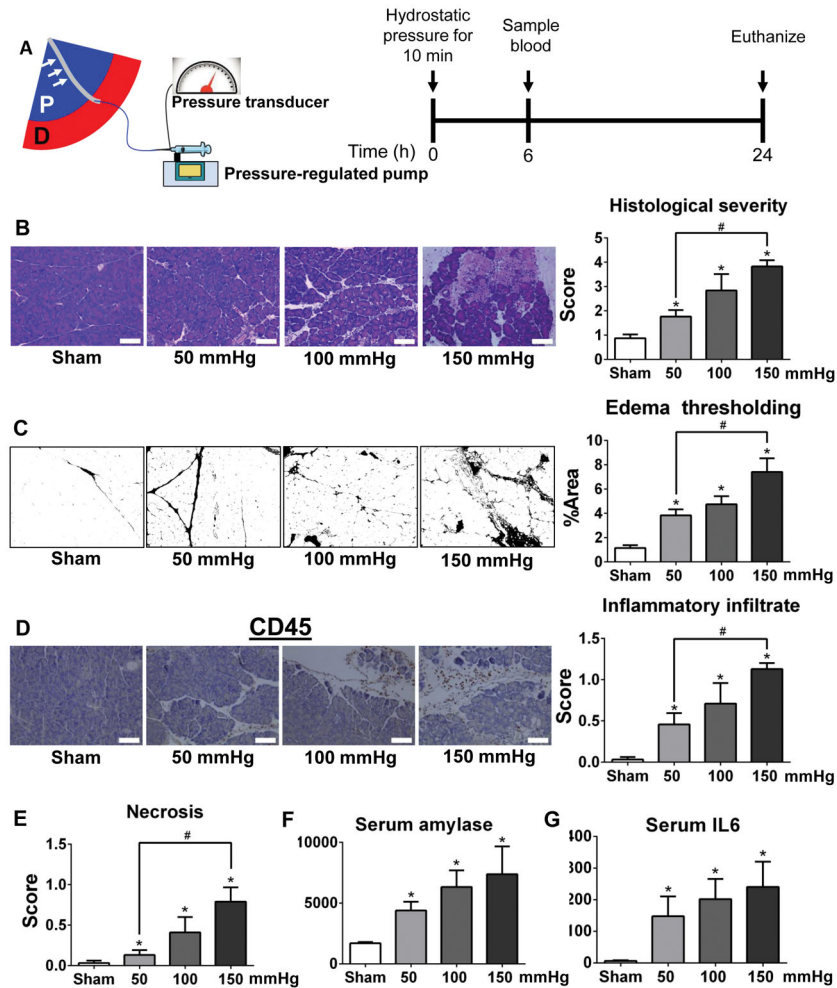


Figure 2. The transient application of high hydrostatic intraductal pressure leads to pancreatitis (A) A schematic of the pressure-regulated pump with pressure monitoring (*left*) and a timeline for assessing pancreatitis severity in this model (*right*). (B) Representative H&E images from sham, 50 mmHg, 100 mmHg, and 150 mmHg, along with overall histological severity scoring from the head of the pancreas. (C) Edema assessed by image thresholding. (D) CD45 immunostaining and subscore for inflammatory infiltrate. (E) Subscoring for necrosis. (F) Serum amylase at 6 h and (G) serum IL6 at 24 h. (n=5–7 mice per condition, *p<0.05, compared to the sham, #p<0.05, compared to 50 mmHg).

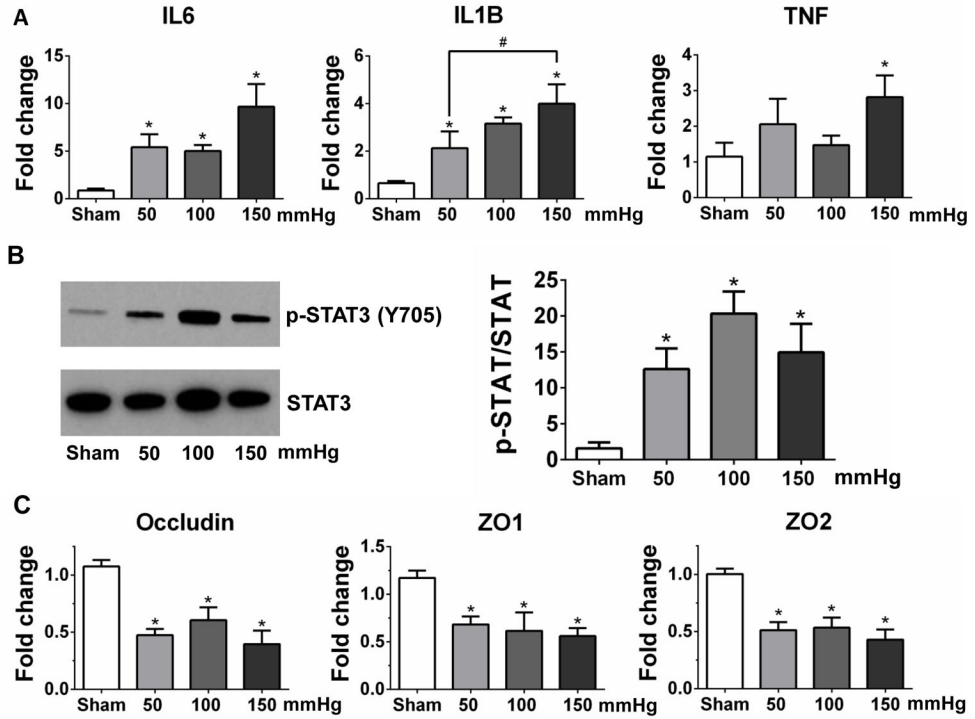


Figure 3. The transient application of hydrostatic intraductal pressure leads to elevations in pancreatic proinflammatory cytokine expression and reductions in tight junction expression (A) Gene expression by RT-qPCR, (B) immunoblotting for phospho-STAT3 (Y705), and (C) expression of genes for tight junction proteins from the pancreatic head 24 h after pressure induction. (n=5–7 mice per condition, *p<0.05, compared to the sham, #p<0.05, compared to 50 mmHg).

Author Manuscript

Author Manuscript

Author Manuscript

Author Manuscript

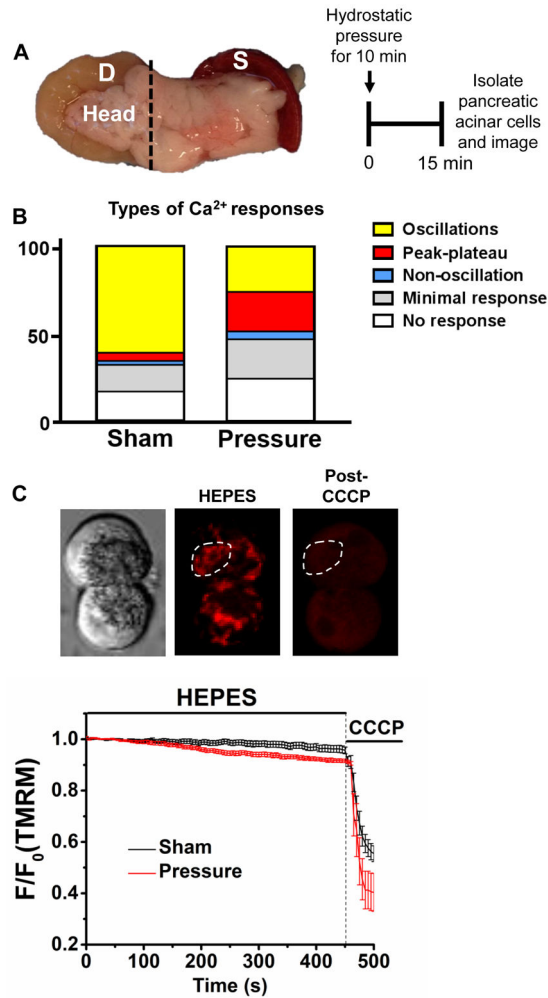


Figure 4. Pressure-induced pancreatitis causes dysregulation of Ca²⁺ processing and a decrease in mitochondrial membrane potential in isolated pancreatic acinar cells
 (A) Image of the pancreas with duodenum (D) and spleen (S) removed en bloc to assist proper identification of the pancreatic head (left) and timeline for pressure induction and pancreatic acinar cell isolation and imaging (right). (B) Histogram shows the proportion of the cells responding as oscillations (yellow), peak-plateau (red), non-oscillation (blue), minimal response (grey), and no response (white) from a sham surgery or pressure induction. (C) Representative image of an acinar cell couplet on the left, transmitted light; middle and right, fluorescent imaging loaded with TMRM to assess mitochondrial membrane potential. The white dashed circle indicates an enriched region of mitochondria that was used for the analysis. Tracing of TMRM from the sham (black) or pressure-induced (red) groups. Data were normalized to the baseline as F/F_0 . (n=10–17 acinar cells, performed from 2–3 mice for each group).

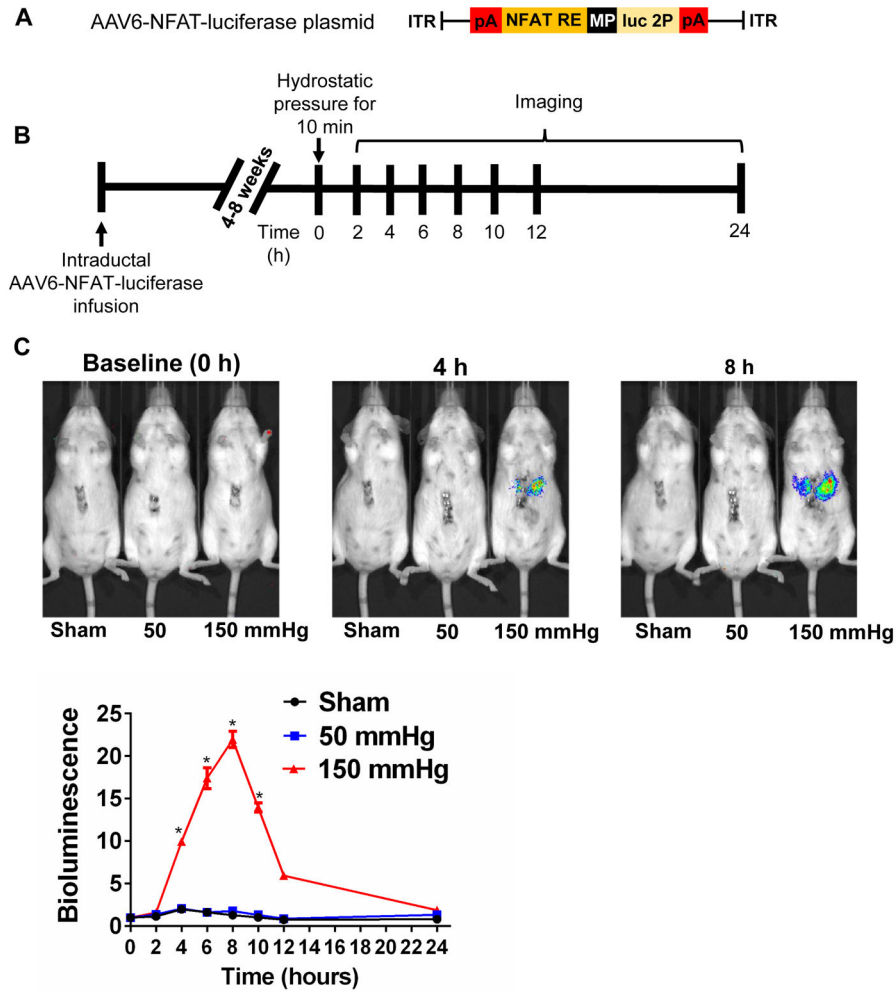


Figure 5. Pressure-induced pancreatitis causes pancreatic calcineurin activation
 (A) Schema for the AAV6-NFAT-luciferase plasmid that we generated. ITR, inverted terminal repeat; RE, response element; pA, poly A; MP, minimal promoter; and luc 2P, luciferase 2P. (B) Timeline for the intraductal infusion of the AAV6, followed by the application of hydrostatic pressure and bioluminescent imaging. (C) Images and quantification of the pancreatic NFAT signal at baseline (time 0), 4, and 8 h after pressure induction. (n=2–3 mice per condition, *p<0.05, compared to the sham at each of respective time point).

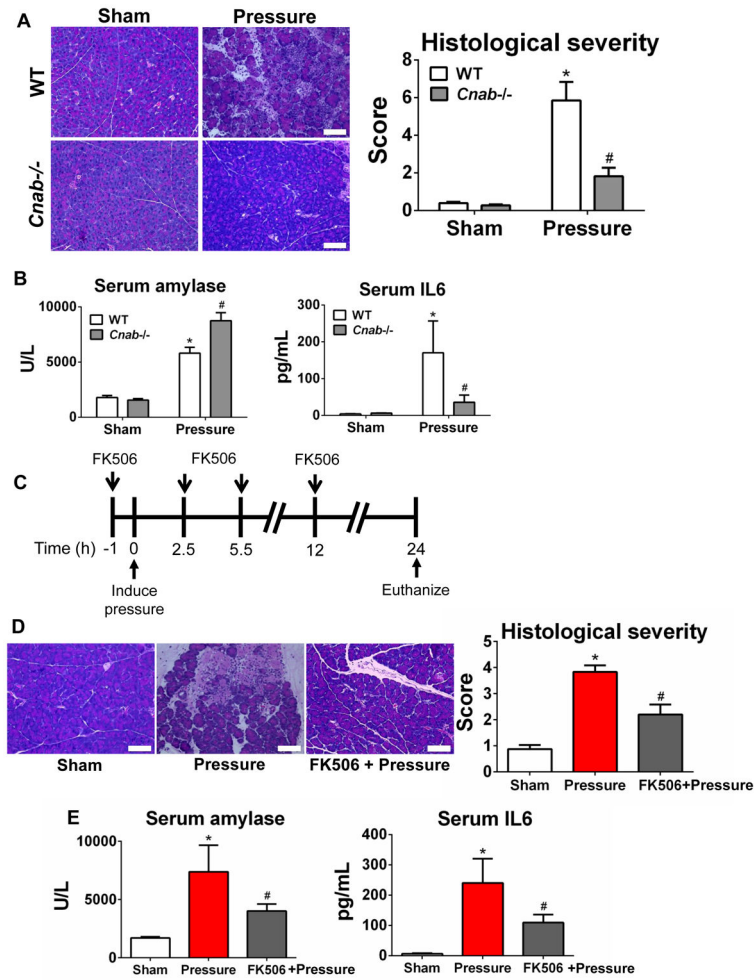


Figure 6. Calcineurin mediates pressure-induced pancreatitis

(A) Representative H&E images from sham and pressure-induced conditions from WT and *Cnab* knockout mice, along with overall histological severity scoring. (B) Serum amylase at 6 h and serum IL6 at 24 h. (C) Timeline for intraperitoneal administration of FK506 (1 mg/kg). (D) Representative H&E images from the sham and pressure-induced conditions, along with overall histological severity scoring. (E) Serum amylase at 6 h and serum IL6 at 24 h. (n=5–7 mice per condition, *p<0.05, compared to the WT sham, #p<0.05, compared to the WT undergoing pressure induction).

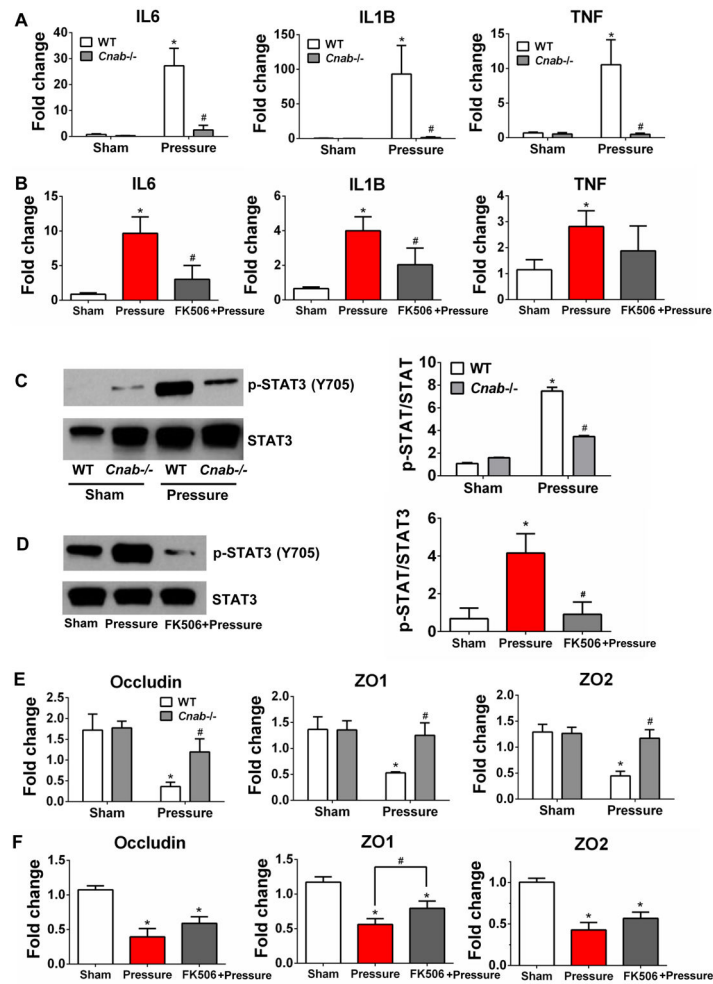


Figure 7. Calcineurin signaling is necessary for pancreatic inflammatory cytokine expression and tight junction integrity in pressure-induced pancreatitis

Gene expression by RT-qPCR from the pancreatic head 24 h after pressure induction in (A) WT versus *Cnab* knockout mice or (B) WT mice receiving FK506 administration. (C, D) Immunoblotting for phospho-STAT3 (Y705) and (E, F) expression of tight junction genes from the pancreatic head 24 h after PIP induction. (n=5–7 mice per condition, *p<0.05, compared to the WT sham, #p<0.05, compared to the WT undergoing pressure induction).